

Fluorescent chemosensor for metal ions based on optically active polybinaphthyls and 1,3,4-oxadiazole

Yan Liu, Lili Zong, Lifei Zheng, Linglin Wu, Yixiang Cheng*

School of Chemistry and Chemical Engineering, Nanjing University, Nanjing 210093, PR China

Received 1 July 2007; received in revised form 16 August 2007; accepted 13 September 2007
Available online 15 September 2007

Abstract

Linear chiral polymers **P-1** and **P-2** were synthesized by the polymerization of (*R*)-5,5'-dibromo-6,6'-di(4-methylphenyl)-2,2'-bis(octoxy)-1,1'-binaphthyl (**R-M-1**) with 2,5-di(4-vinylphenyl)-1,3,4-oxadiazole (**M-2**) and 2,5-di(4-tributylstannylphenyl)-1,3,4-oxadiazole (**M-3**) via Heck and Stille cross-coupling reaction, respectively. The chiral conjugated polymer **P-1** can show strong green-blue fluorescence, and the chiral polymer **P-2** shows strong blue fluorescence. While the conjugated polymers **P-1** and **P-2** were used as fluorescent chemosensor for metal ions, their fluorescence can be efficiently quenched on the addition of different metal ions. The obvious quenching effect of the polymers **P-1** and **P-2** indicates that the intramolecular photoinduced electron transfer (PET) or photoinduced charge transfer (PCT) between the polymer backbone and receptor-ions in the main chain of fluorescent chemosensor can lead to the pronounced fluorescence quenching. The results also show that the chiral polymers **P-1** and **P-2** incorporating 1,3,4-oxadiazole moiety as the recognition site can act as a special fluorescent chemosensor for the appropriate detection of the sensitive and selective sense of metal ions.

© 2007 Elsevier Ltd. All rights reserved.

Keywords: (*R*)-BINOL; Chiral conjugated polymer; Fluorescent chemosensor

1. Introduction

Organic conjugated polymer based on π -conjugated organic molecules and regular arrangement of polymer chains has still been attracting much interest during the past decade. These functional polymers with tunable optical and electronic properties can be achieved by the careful combination of the designed monomers. They can also be used to prepare organic light-emitting diodes, electroluminescent devices, nonlinear optical materials, supramolecular sensors and full-color flat panel displays [1–4]. Fluorescent chemosensors are dye molecules whose fluorescence excitation/emission changes in response to the surrounding medium or through specific molecular recognition events. Due to their simplicity and high sensitivity, fluorescent sensors have been widely utilized as popular tools for chemical, biological, and medical

applications [5–8]. The most general strategy for fluorescent sensor design is to combine fluorescent dye molecules with designed receptors for specific analytes, so that the recognition event between receptor and analyte can lead to a fluorescence property change of the dye moiety. On the basis of the concepts provided by host–guest chemistry, cation sensing has recently risen to a dominant position in research devoted to the detection of designated species. One of the keys in designing a useful chemosensor is to effectively convert molecular recognition into optical signals. Most of the fluorescent chemosensors for cations are composed of a cation recognition unit (ionophore) together with a fluorogenic unit (fluorophore) and are called fluoroionophores. An effective fluorescent chemosensor must convert the event of cation recognition by the ionophore into an easily monitored and highly sensitive optical signal from the fluorophore [9,10]. Fluorescent conjugated polymers have several advantages over small molecule sensors due to enhancements associated with electronic communication between receptors along the polymer backbone, processability, and ease of structural modification. The conjugated

* Corresponding author. Tel.: +86 25 83592709; fax: +86 25 83317761.
E-mail address: yxcheng@nju.edu.cn (Y. Cheng).

polymers incorporating molecular recognition moieties are that they can make use of the high sensitivity of conjugated polymers to external structural perturbations and to electron density changes within the conjugated polymer main backbone, when they can interact and form complexes with metal ions [11–13].

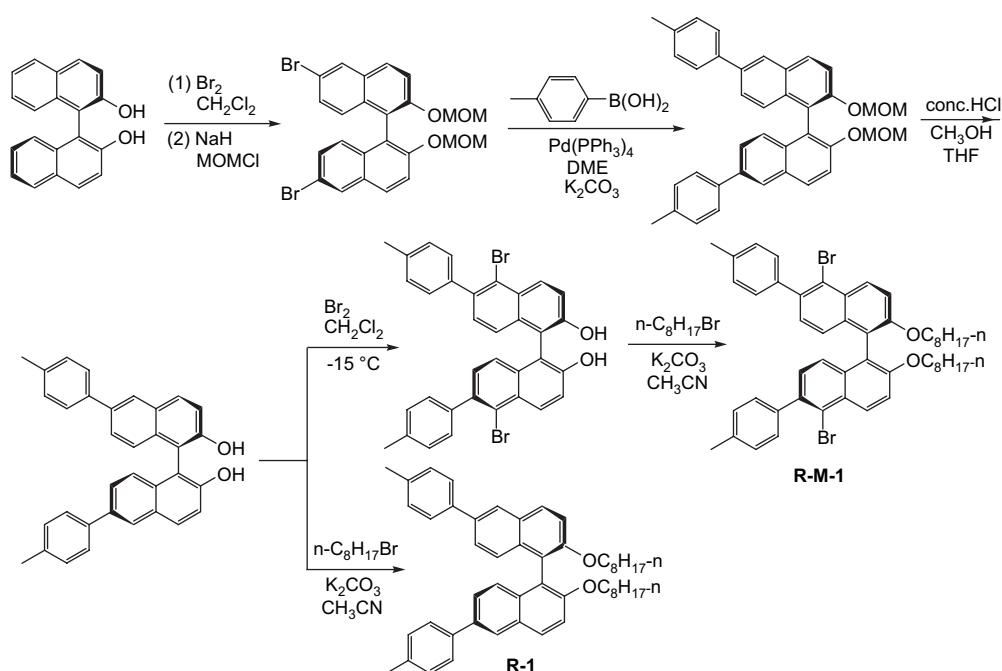
The conjugated polymers incorporating optically active binaphthyl moiety in the main chain can exhibit a sort of excellent fluorescent material with good fluorescence quantum efficiencies due to the extended π -electronic structure between the chiral repeating unit and the conjugated linker. These rigid and regular chiral binaphthyl-based polymers have represented a new generation of materials for applications in areas such as fluorescence sensors in chiral molecule recognition and electro-optical materials [14–19]. According to the previous literatures, the skeletal structure of BINOL could be selectively functionalized at 3,3'- or 6,6'-positions of binaphthyl, so far there has not been report on the polymer based on optically active binaphthyl at 5,5'-positions to form the linear polybinaphthyls main-chain backbone. In this paper, we report the bromination of (*R*)-6,6'-di(4-methylphenyl)-2,2'-binaphthol at 5,5'-positions of BINOL in a mild condition for the direct and facile synthesis of (*R*)-5,5'-dibromo-6,6'-di(4-methylphenyl)-2,2'-binaphthol. (*R*)-5,5'-Dibromo-6,6'-di(4-methylphenyl)-2,2'-bisoxetoxy-1,1'-binaphthyl (*R*-**M-1**) can be directly obtained by the etherization of hydroxyl groups of (*R*)-5,5'-dibromo-6,6'-di(4-methylphenyl)-2,2'-binaphthol with *n*-C₈H₁₇Br. The linear polymers **P-1** and **P-2** can be synthesized by the polymerization of *R*-**M-1** with 2,5-di(4-vinylphenyl)-1,3,4-oxadiazole (**M-2**) and 2,5-di(4-tributylstannylphenyl)-1,3,4-oxadiazole (**M-3**) via Heck and Stille reaction, respectively. Conjugated polymers containing 1,3,4-oxadiazole moiety are one of the most widely used electron transporting and hole

blocking materials in LED devices and LED blends because oxadiazole unit combined with the advantage of the excellent properties on the better chromophore, high thermal and oxidative stability, and the good charge injection and transporting building blocks [1,20–24]. The polymer **P-1** has strong green-blue fluorescence, and the polymer **P-2** can show strong blue fluorescence. Moreover, this neutral ligand 1,3,4-oxadiazole can coordinate with different transition metal ions to form polymer complexes. While the polymers **P-1** and **P-2** were used as fluorescent chemosensor for metal ions, their fluorescence can be efficiently quenched on the addition of different metal ions. The results indicate that the polymer **P-1** can show more sensitive and selective sense of metal ions Ni²⁺, Cu²⁺, Pb²⁺, Zn²⁺, Hg²⁺, and Ag⁺ than the polymer **P-2**. Such distinct ion responsive behaviors also reveal the obvious difference of two chiral polymer backbone structures.

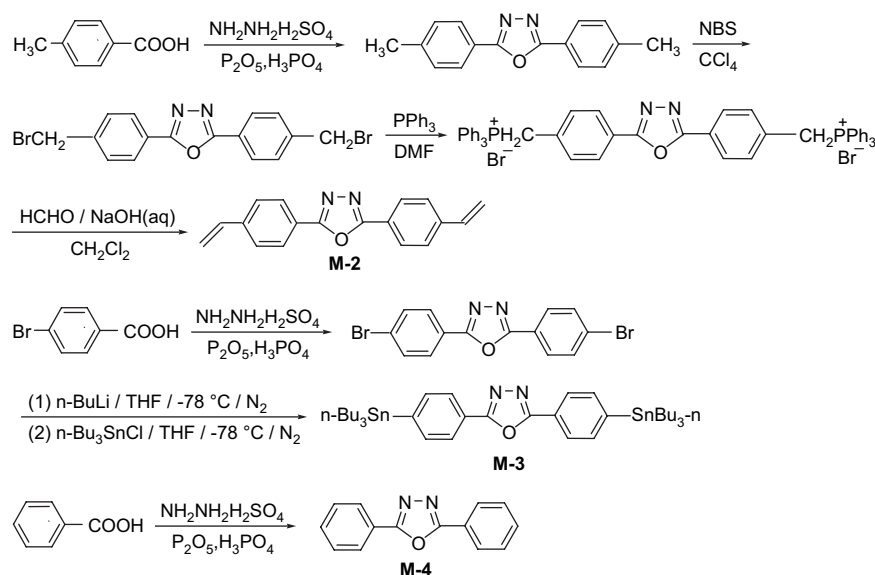
2. Results and discussion

2.1. Syntheses and features of the monomers and polymers

4-Methylphenylboronic acid was synthesized according to the literature [25–27]. (*R*)-6,6'-Dibromo-2,2'-binaphthol and (*R*)-6,6'-dibromo-2,2'-bis(methoxymethoxy)-1,1'-binaphthyl were prepared and purified as per the reported literatures [28–32]. The chiral repeating unit *R*-1 and the monomer *R*-**M-1** were synthesized from (*R*)-BINOL (Scheme 1), and 2,5-di(4-vinylphenyl)-1,3,4-oxadiazole (**M-2**), 2,5-di(4-tributylstannylphenyl)-1,3,4-oxadiazole (**M-3**) and the repeating unit 2,5-diphenyl-1,3,4-oxadiazole (**M-4**) were prepared as per the reported literatures (Scheme 2) [22–24,33–36].



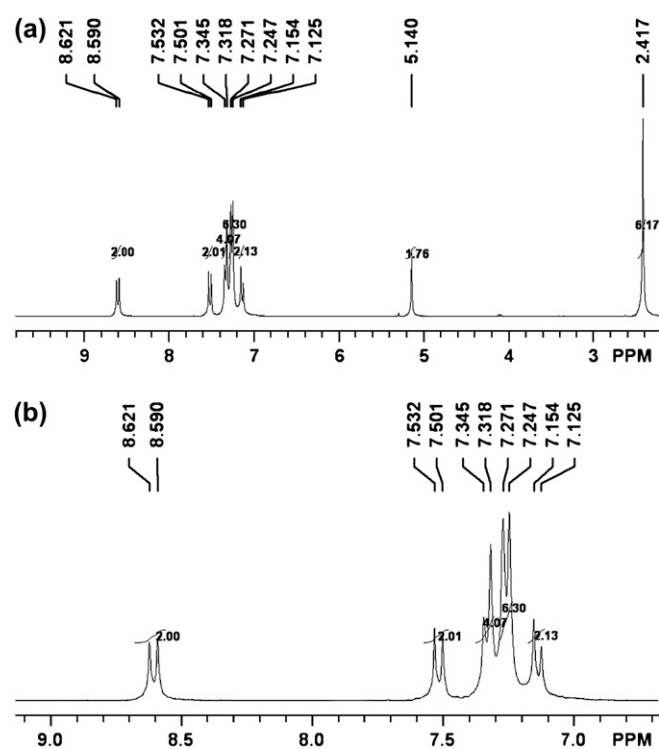
Scheme 1. Synthesis procedures of *R*-**M-1** and the chiral repeating unit *R*-1.

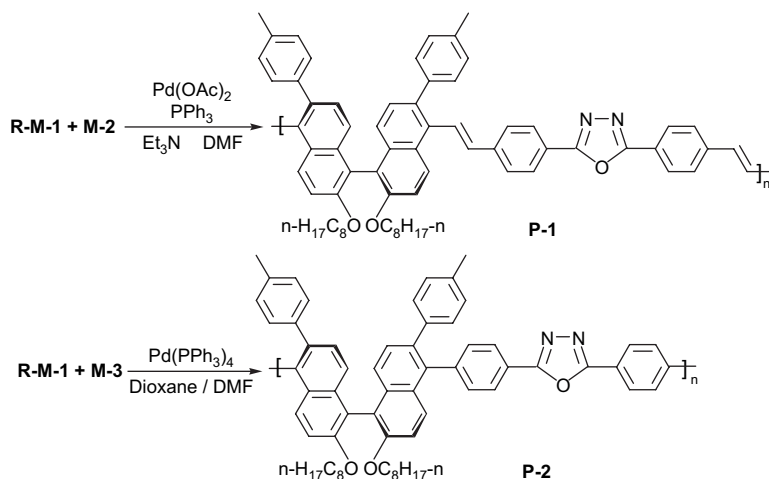
Scheme 2. Synthesis procedures of **M-2**, **M-3**, and the repeating unit **M-4**.

Optically active 2,2'-binaphthol (BINOL) have often been used as the starting materials for the preparation of the conjugated polymers that have a main-chain chiral configuration. According to the reported literatures, the skeletal structure of BINOL can be selectively halogenated at the 3,3'-or 6,6'-positions of 2,2'-binaphthol, leading to a variety of binaphthyl derivatives [29,30,37–39]. So far there has not been report on halogenation of BINOL at 5,5'-positions except that Shimada and Lemaire reported the direct and facile synthesis of 5,5'-diiodo-/5,5'-dibromo-2,2'-bis(diphenylphosphino)-1,1'-binaphthyl (BINAP), and Pirkle described the synthesis of 5,5'-dibromo-6,6',7,7'-tetramethyl-2,2'-binaphthol [40–42]. But when the 4,4'-positions of BINOL were occupied by bromine atoms, additional bromination occurred at the 6,6'-positions to give 4,4',6,6'-tetrabromo-2,2'-binaphthol [43–45]. Based on Lin's and Pu's reports, the bromination substitution could undergo at the 4,4'-positions while 6,6'-positions of BINOL were occupied by chlorine atoms and hydroxyl groups of BINOL were etherized by ethyl groups [28,46–48]. In our study, (*R*)-BINOL can be specifically brominated at 5,5'-positions in a mild condition to afford a pure product in an excellent yield of 83% when 6,6'-positions are occupied by 4-methylphenyl groups. Fig. 1 shows ^1H NMR of (*R*)-5,5'-dibromo-6,6'-di(4-methylphenyl)-2,2'-binaphthol. Chemical shifts of 5,5'-position protons in ^1H NMR of (*R*)-6,6'-di(4-methylphenyl)-2,2'-binaphthol appears at 8.08 ppm. But this single peak disappears in the ^1H NMR of (*R*)-5,5'-dibromo-6,6'-di(4-methylphenyl)-2,2'-binaphthol, from which it can be concluded that bromination occurs at 5,5'-positions of BINOL. To our knowledge, it is the direct and facile bromination of BINOL at 5,5'-positions so far. Starting from the bromination of BINOL at 5,5'-positions, we can further design and synthesize a series of the novel binaphthyl-based chiral ligands by strategic placement of substituents within the framework of a given BINOL derivative. These chiral ligands based on steric and electronic properties can be modified at the well-

defined molecular level, which will lead to the outcome of a new generation of novel binaphthyl-based materials for applications in asymmetric catalysis, chiral sensors and electro-optical devices.

R-M-1 can be served as the monomer for the synthesis of the desired chiral polymers **P-1** and **P-2** with the linear main-chain backbones. Here, the typical Heck and Stille reaction conditions were applied to the polymerization (Scheme 3) [49–55]. The polymerization could be produced in good yields of 80.1% and 87.3%, respectively. The GPC results of

Fig. 1. ^1H NMR of (*R*)-5,5'-dibromo-6,6'-di(4-methylphenyl)-2,2'-binaphthol.

Scheme 3. Synthesis procedures of **P-1** and **P-2**.

the polymers **P-1** and **P-2** show the moderate molecular weight (Table 1). The octoxy and 4-methylphenyl group substituents on binaphthyl ring as the side chain of the polymer can not only improve solubility in common organic solvents, but also modify the electronic properties and conjugated structure of chiral polymer. Herein, an electron-deficient heterocyclic unit, 1,3,4-oxadiazole as the conjugated molecular linker and recognition site of fluorescent chemosensor was introduced into the main-chain backbone of chiral conjugated polymers to improve the electron transporting properties of the polymer and increase the stability of the resulting chiral polymers **P-1** and **P-2**. But so far, there are few reports on 1,3,4-oxadiazole unit as the precursor into the chiral conjugated polybinaphthyls main chain [22–24]. The chiral conjugated polymers **P-1** and **P-2** can show strong fluorescence and directly coordinate with metal ions to form the metal–polymer complexes. In our study, while the conjugated polymers **P-1** and **P-2** were used as fluorescent chemosensor for metal ions, their fluorescence can be efficiently quenched on the addition of different metal ions.

P-1 and **P-2** are air stable solids with dark green color and show good solubility in THF, CH_2Cl_2 , CHCl_3 and DMF. The nonplanarity of the polymer in the main-chain backbone and flexible octoxy and 4-methylphenyl group substituents on binaphthyl unit can render the chiral polymer soluble in common organic solvents. **P-1** shows a glass transition temperature (T_g) at 111 °C, but **P-2** shows no glass transition temperature (T_g). Thermogravimetric analyses (TGA) of two polymers were carried out under a N_2 atmosphere at a heating rate of 10 °C/min. According to Fig. 2, the TGA plot of **P-1** is

Table 1
Polymerization results and characterization of **P-1** and **P-2**

	Yield (%)	M_w^a	M_n^a	PDI	$[\alpha]_D^b$
P-1	80.1	8970	8930	1.01	+154.0
P-2	87.3	25,220	19,280	1.31	+120.0

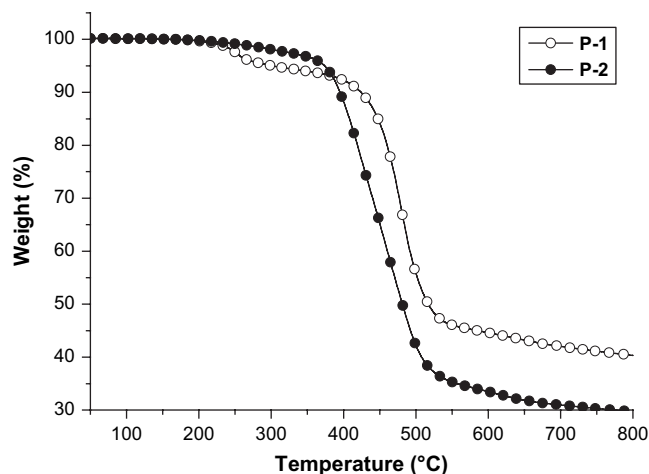
^a M_w , M_n and PDI of **P-1** and **P-2** were determined by gel permeation chromatography using polystyrene standards in THF.

^b Temperature at 20 °C and solvent in CH_2Cl_2 ($c = 0.10$).

different from that of **P-2**, and **P-2** has higher thermal stability than **P-1**. **P-1** exhibits two-step degradation process, first step degradation is observed at temperature ranging from 210 to 425 °C. There is about 6% loss of weight. The second step degradation appears at temperature ranging from 430 to 560 °C. **P-1** tends to complete decomposition before 750 °C. A total loss of about 60% is observed when heated to 800 °C. But **P-2** appears an apparently one-step degradation at temperature ranging from 365 to 650 °C, and tends to complete decomposition at 750 °C. A total loss of about 70% is observed when heated to 800 °C.

2.2. Optical properties

Figs. 3 and 4 illustrate the UV–vis absorption spectra and fluorescent spectra of the linker repeating units **M-2** and **M-4**, the chiral repeating unit **R-1** and the polymers **P-1** and **P-2** in THF. Optical properties of the repeating unit and the polymers are summarized in Table 2. Compared to the repeating unit **R-1** and the linker repeating units **M-2**, **M-4**, UV–vis absorption spectra of the conjugated polymers show greater red shift. UV absorption maxima λ_{max} of **M-2**, **M-4** and **R-1** appear at

Fig. 2. TGA curves of **P-1** and **P-2**.

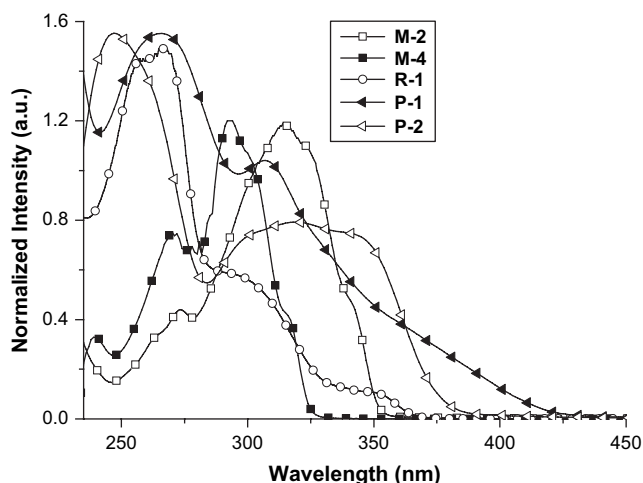


Fig. 3. UV-vis spectra of M-2, M-4, R-1, P-1 and P-2 in THF.

314, 292 and 267 nm, respectively. The absorption wavelengths λ_{max} of P-1 and P-2 appear at 307 and 322 nm in THF solution. But both P-1 and P-2 show stronger and broader absorption in the region from 280 to 380 nm. It can be concluded that there is a large red shift in the electronic absorptions of conjugated polymers due to the effective $\pi-\pi^*$ conjugated segment of the linker conjugated unit M-2 or M-4 and the chiral repeating unit R-1 in the linear main chain of the polymers P-1 and P-2 [14,15,23,56].

According to Table 2 and Fig. 4, M-2, M-4 and the chiral repeating unit R-1 can show double band fluorescence in ultraviolet region. The fluorescent wavelength $\lambda_{\text{max}}^{\text{F}}$ of P-2 appears at 423 nm, but P-1 shows greater red shift to 468 nm. The fluorescent efficiency (Φ_{PL}) of P-1 and P-2 are 0.61 and 0.23, respectively. It can be concluded that the polymer P-1 has strong fluorescence with higher fluorescence quantum efficiency due to the more extended π -electronic structure between R-1 and the conjugated linker M-4 via vinylene bridge [15,23,24,57]. Furthermore, 4-methylphenyl branches at 6,6'-positions of 1,1'-binaphthyl moieties can act as the polymer light absorbing antenna. This light harvesting effect

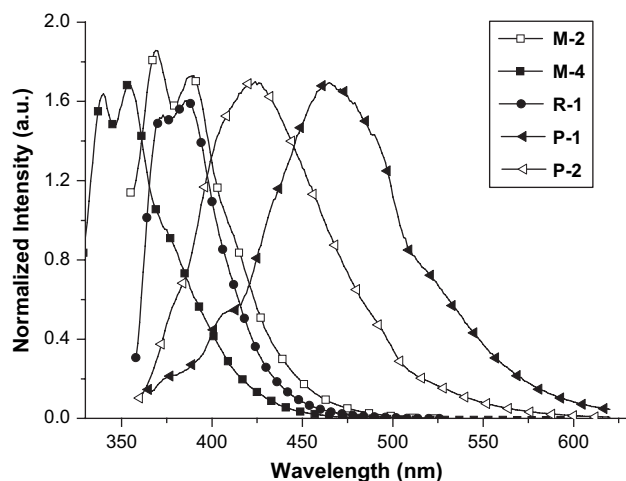


Fig. 4. Fluorescent spectra of M-2, M-4, R-1, P-1, and P-2 in THF.

Table 2
Optical data of M-1 and M-4, R-1 and polymers

	UV-vis (λ_{max})	PL (λ_{max})		Stokes shift ^a	Φ_{PL} ^b
		λ_{ex}	λ_{em}		
M-1	314	350	369, 389		
M-4	292	314	340, 354		
R-1	267	353	373, 385		
P-1	307	359	468	161	0.61
P-2	322	353	423	101	0.23

^a Stokes shift = PL λ_{max} (nm) - UV-vis λ_{max} (nm).

^b These values were estimated by using the quinine sulfate solution (ca. 1.0×10^{-5} M) in 0.5 M H₂SO₄ ($\Phi_{\text{f}} = 55\%$) as a standard.

can also enhance the fluorescence of the linear conjugated polymers due to an efficient intramolecular energy migration from the light absorbing antenna to the conjugated polymers' main chain. The greatly enhanced fluorescence of the chiral conjugated polymers P-1 and P-2 is expected to have the potential application in the polarized light-emitting materials and fluorescent chemosensor for the detection of the sensitive and selective sense of transition metal ions.

2.3. CD spectra

The specific rotation value ($[\alpha]_{\text{D}}^{25}$) of the chiral repeating unit R-1 is -67.3 (c 0.68, CH₂Cl₂), and $[\alpha]_{\text{D}}^{25}$ values of the polymers P-1 and P-2 are $+154.0$ (c 0.1, CH₂Cl₂) and $+120.0$ (c 0.03, CH₂Cl₂), and have the opposite signal with the chiral repeating unit R-1. As a result, the chiral polymer is made of optically pure 1,1'-binaphthyl units. Both the chiral repeating unit R-1 and the chiral polymers P-1 and P-2 exhibit intense CD signals with negative and positive Cotton effect in their CD spectra (Fig. 5). CD spectral data of the chiral repeating unit R-1 and the polymers are listed in Table 3. ¹L_a and ¹B_b band positions of the polymers P-1 and P-2 are almost similar as the chiral repeating unit R-1, but CD intensity of the chiral repeating unit R-1 appears more than twice the magnitude as that of polymers P-1 and P-2. The chiral polymers P-1 and P-2 do not appear the long-wavelength Cotton effect. This result may be attributed to the linear structure of

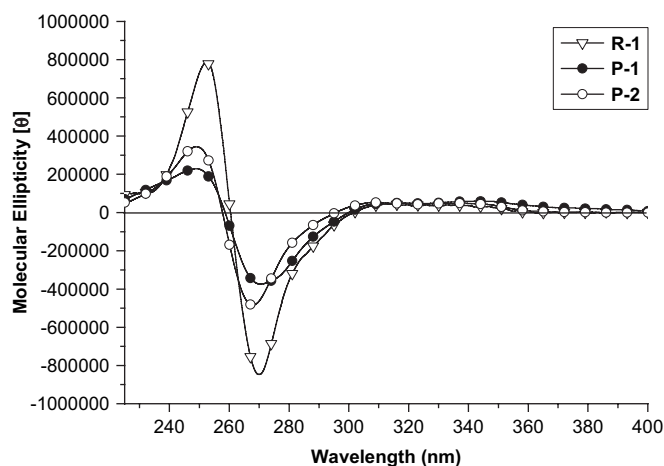


Fig. 5. CD spectra of R-1, P-1, and P-2.

Table 3
CD spectral data of the chiral repeating unit *R*-1 and polymers

	<i>R</i> -1 × 10 ⁵	<i>P</i> -1 × 10 ⁵	<i>P</i> -2 × 10 ⁵
[θ]	+7.88 (252.2)	+2.36 (249.0)	+3.47 (249.0)
(λ _{max} in nm)	-8.48 (270.1)	-3.73 (270.7)	-4.89 (267.3)

polybinaphthyls at 5,5'-position. According to Pu's and our previous reports [58,59], if optically active polybinaphthyls do not have a propagating helical chain conformation in solution, the specific rotation and CD spectrum of this kind of polymer are very close to those of its monomeric model compound. In this paper, the chiral polymers *P*-1 and *P*-2 adopt the linear main-chain backbone due to the polymer chain at 5,5'-positions of 1,1'-binaphthyl, which has the similar chain backbone as the 4,4'-positions polymer of 1,1'-binaphthyl [60].

2.4. Responsive properties on metal ions

The effects of the molecular recognition sites in optically active polybinaphthyl-based conjugated polymers *P*-1 and *P*-2 on metal ion sensing have been investigated (Figs. 6 and 7). The influences of various metal ions on the fluorescence emission response of the polymer are shown in Table 4. The concentrations of *P*-1 and *P*-2 corresponding to 1,3,4-oxadiazole receptor units were fixed at 1.0 × 10⁻⁵ M. The selectivity of the chemosensor for metal cations was examined. Ni²⁺,

Cu²⁺, Pb²⁺, Zn²⁺, Hg²⁺, Ag⁺ ions were used at a concentration of 6.0 × 10⁻⁴ M. Fluorescence quenching behavior of *P*-1 and *P*-2 with various molar ratios of metal salts was also investigated to examine the effect of the chelating ability on the fluorescence quenching property of the 1,3,4-oxadiazole group in the polymers. The fluorescence quenching ratios of *P*-1 are 39.3, 36.2, 36.6, 39.2, 34.5, and 33.7% by Ni²⁺, Cu²⁺, Pb²⁺, Zn²⁺, Hg²⁺, and Ag⁺ ions upon the 1:1 molar ratio addition of a metal salt solutions, while that of *P*-2 are 23.2, 22.3, 19.1, 26.7, 23.3, and 24.3%, respectively. The obvious quenching effect of *P*-1 and *P*-2 to metal ions can be ascribed to intramolecular photoinduced electron transfer (PET) or photoinduced charge transfer (PCT) between the polymer backbone and receptor-ions in the main chain of fluorescent chemosensor [61–64].

The quenching efficiency is related to the Stern–Volmer constant, *K*_{sv}, and is determined by monitoring measurable changes in the fluorescence via the Stern–Volmer equation: *I*₀/*I* = 1 + *K*_{sv}[*Q*] (Fig. 8). Here *I*₀ is the fluorescence emission intensity in the absence of the quencher, *I* is the fluorescence emission intensity in the presence of the quencher, and [*Q*] is the quencher concentration, that is metal ion's concentration. *K*_{sv} constants of the polymer *P*-1 to metal ions are bigger than that of *P*-2 (Table 3), which indicates that the polymer *P*-1 can show more sensitive and selective sense of metal ions Ni²⁺, Cu²⁺, Pb²⁺, Zn²⁺, Hg²⁺ and Ag⁺ than the polymer *P*-2. Such distinct ion responsive behaviors revealed the

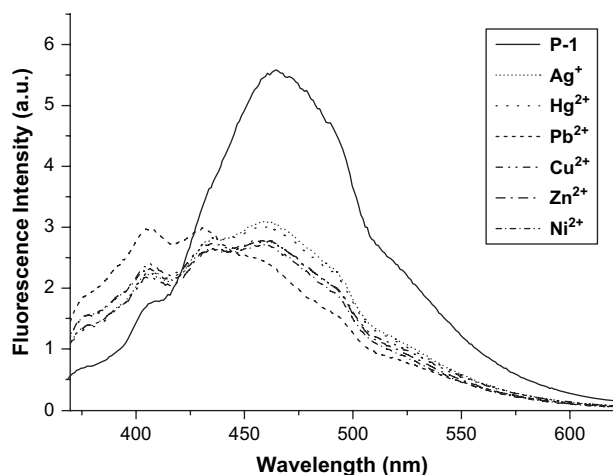


Fig. 6. Emission spectra of metal–polymer complexes for *P*-1 at the ratio of 1:1 (λ_{ex} = 359 nm).

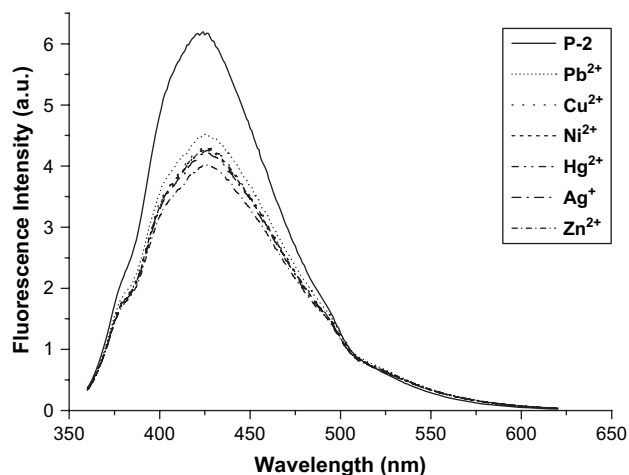


Fig. 7. Emission spectra of metal–polymer complexes for *P*-2 at the ratio of 1:1 (λ_{ex} = 353 nm).

Table 4
The quenching ratio (%) and average *K*_{sv} of the transition metal ions to *P*-1 and *P*-2

	<i>P</i> -1 (<i>n</i> _{ion} : <i>n</i> _{<i>P</i>-1})						<i>P</i> -2 (<i>n</i> _{ion} : <i>n</i> _{<i>P</i>-2})						<i>K</i> _{SV} × 10 ⁴ (M ⁻¹)	
	1:0.2	1:0.5	1:0.8	1:1	1:2	1:5	1:0.2	1:0.5	1:0.8	1:1	1:2	1:5	<i>P</i> -1	<i>P</i> -2
Ag ⁺	25.5	27.5	29.8	33.7	38.6	48.8	13.7	17.5	18.3	24.3	33.9	52.1	8.78	4.55
Hg ²⁺	26.1	29.4	31.4	34.5	39.7	48.7	11.7	16.4	21.5	23.3	34.3	52.0	9.23	4.26
Pb ²⁺	19.5	28.5	31.8	36.6	39.9	45.4	5.96	12.7	16.7	19.1	30.2	55.7	7.92	2.74
Cu ²⁺	24.2	26.0	32.2	36.2	40.9	50.8	11.4	15.1	20.1	22.3	32.3	51.2	8.64	3.99
Ni ²⁺	33.3	35.4	37.9	39.3	44.2	54.6	11.3	15.9	20.0	23.2	28.9	50.2	12.3	4.07
Zn ²⁺	33.0	35.1	36.8	39.2	41.3	54.2	12.9	18.1	24.1	26.7	36.6	53.4	12.5	4.85

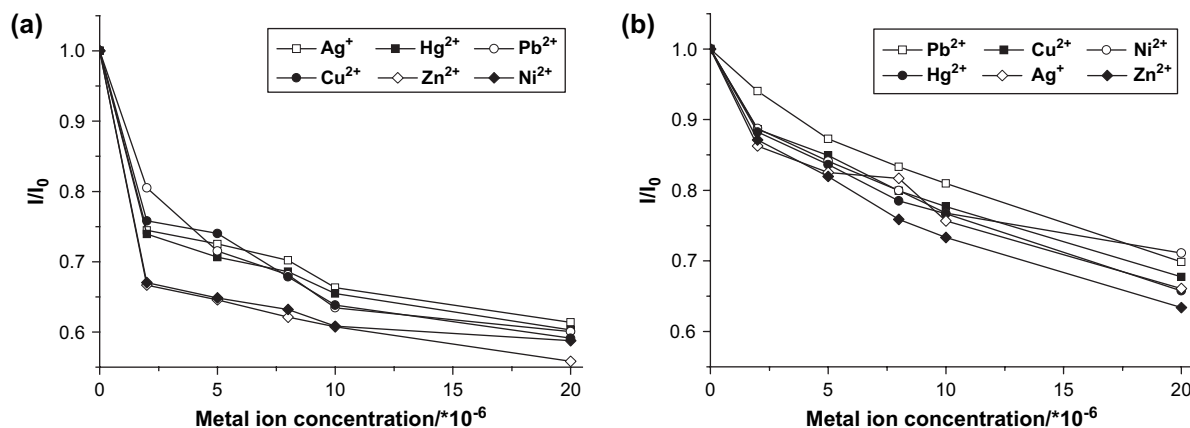


Fig. 8. The quenching ability of metal ions for **P-1** (a) and **P-2** (b).

obvious difference of two chiral polymer backbone structures. It can also be found that the emission wavelengths of all metal–polymer complexes of **P-2** do not produce an obvious change from metal-free polymer, but the fluorescent wavelengths and spectra of **P-1** show an obvious difference upon addition of a metal ion solution. The maximum emission wavelength $\lambda_{\text{max}}^{\text{F}}$ of **P-1** at 468 nm appears blue-shifted to the region of 460–430 nm. On the contrary, the weak emission wavelengths of **P-1** at 406 nm show an obvious fluorescent enhancement upon the addition of a metal salt solution.

3. Conclusions

The linear conjugated polymers **P-1** and **P-2** based on chiral polybinaphthyls at 5,5'-positions show strong fluorescence due to the extended π -electronic structure between the chiral repeating unit **R-1** and the conjugated linker **M-4**. While the conjugated polymers **P-1** and **P-2** were used as fluorescent chemosensor for metal ions, their fluorescence can be efficiently quenched on the addition of different metal ions. The obvious quenching effect of **P-1** and **P-2** to metal ions can be ascribed to intramolecular photoinduced electron transfer or photoinduced charge transfer between the polymer backbone and receptor-ions in the main chain of fluorescent chemosensor. The results indicate that the polymer **P-1** can show more sensitive and selective sense of metal ions Ni²⁺, Cu²⁺, Pb²⁺, Zn²⁺, Hg²⁺ and Ag⁺ than the polymer **P-2**. It may provide the critical information for the design of novel and sensitive chemosensory materials.

4. Experimental section

4.1. General

¹H and ¹³C NMR spectra measurements (all in CDCl₃) were recorded on a 300-Bruker spectrometer with TMS as an internal standard. FT-IR spectra were recorded on a Nexus 870 FT-IR spectrometer. UV–vis spectra were obtained from a Perkin–Elmer Lambda 25 spectrometer. DSC–TGA was performed on a Perkin–Elmer Pyris-1 instrument under a N₂

atmosphere. Fluorescent spectra were obtained from a 48000 DSCF spectrometer. MS was determined on a Micromass GCT. Specific rotation was determined with a Ruolph Research Analytical Autopol I. C, H, and N of elemental analyses were performed on an Elementar Vario MICRO analyzer. The circular dichroism (CD) spectrum was determined with a Jasco J-810 spectropolarimeter. Molecular weight was determined by gel permeation chromatography (GPC) with Waters-515 HPLC pump and THF was used as solvent and relative to polystyrene standards. All solvents and reagents were commercially available A.R. grade. (*R*)-2,2'-Binaphthol (BINOL) were purchased from Aldrich and directly used without purification. All reactions were performed under a N₂ atmosphere using Schlenk techniques. THF and Et₃N were purified by distillation from sodium in the presence of benzophenone. CH₂Cl₂ and CH₃CN were distilled from P₂O₅.

Metal ion titration: Each metal ion titration experiment was started with 4.0 mL of polymer in THF solution with a known concentration (1.0×10^{-5} M). Solution of metal salt (acetate or chloride, 6.0×10^{-4} M) was used for the titration. Polymer–metal complexes were produced by adding aliquots of a solution of the selected metal salt to a THF solution of the chiral polymer (4.0 mL). The mixture was stirred constantly during the titration. Steady-state fluorescent spectra were monitored 15 min after addition of the metal salt to the polymer solution.

4.2. Preparation of the monomer **R-M-1**

(*R*)-6,6'-Dibromo-2,2'-bis(methoxymethoxy)-1,1'-binaphthyl (0.96 g, 1.80 mmol) and Pd(PPh₃)₄ (208.2 mg, 0.180 mmol) were mixed in DME (15 mL) under a N₂ atmosphere. 4-Methylphenylboronic acid (0.86 g, 6.32 mmol) and 2 M K₂CO₃ solution (4.7 mL) were added to the above solution. The resulting mixture was stirred and refluxed for 10 h under a N₂ atmosphere. The solution was gradually cooled to room temperature, and the solution was filtered through a short column of silica gel with ethyl acetate as an eluent. After removal of solvents under reduced pressure, the residue was extracted with CH₂Cl₂ (2 × 40 mL) and washed with water and brine twice

and then dried over anhydrous Na_2SO_4 . After removal of solvent, the crude product (*R*)-6,6'-di(4-methylphenyl)-2,2'-bis(methoxymethoxy)-1,1'-binaphthyl was further purified by column chromatography (petroleum ether/ethyl acetate) (15:1 v/v) to afford a pure solid product (730 mg, 73% yield). The product was dissolved in mixed solvents of 10 mL THF and 10 mL methanol. Fifteen millilitres of HCl (12 M) solution was added to the above solution. The solution was kept stirring at room temperature for 8 h. After the removal of all solvents under reduced pressure, the residue was extracted with ethyl acetate (2×30 mL) and washed with 2 M K_2CO_3 solution and brine twice, and dried over anhydrous Na_2SO_4 . After removal of solvent, a pure solid product (*R*)-6,6'-di(4-methylphenyl)-2,2'-binaphthol was obtained in the yield of 93.3% (573 mg); Mp: 113–116 °C; $[\alpha]_{\text{D}} = -288.2$ (*c* 0.5, CH_2Cl_2). ^1H NMR (CDCl_3): δ 8.08 (s, 2H), 8.02–8.05 (d, 2H, $J = 8.9$ Hz), 7.55–7.58 (d, 6H, $J = 8.0$ Hz), 7.40–7.43 (d, 2H, $J = 8.9$ Hz), 7.26–7.24 (m, 6H), 5.12 (s, 2H), 2.40 (s, 6H). ^{13}C NMR (CDCl_3): δ 153.1, 138.3, 137.5, 137.3, 132.8, 132.1, 130.2, 130.0, 127.6, 127.5, 126.4, 125.1, 118.6, 111.1, 21.6. FT-IR (KBr, cm^{-1}): 3500.3, 3423.8, 3021.4, 2918.2, 1596.9, 1500.6, 1471.8, 1383.5, 1355.9, 1286.5, 1217.5, 1189.3, 1173.4, 1148.6, 1128.3, 935.3, 889.5, 812.5.

Bromine (0.30 mL, 5.79 mmol in 10 mL CH_2Cl_2) was slowly added to a solution of (*R*)-6,6'-di(4-methylphenyl)-1,1'-binaphthol (540 mg, 1.16 mmol) in CH_2Cl_2 (10 mL) at -15 °C over 1 h. The solution was stirred overnight and gradually warmed to room temperature. The reaction was quenched with 10% aqueous $\text{Na}_2\text{S}_2\text{O}_3$ (20 mL). After removal of solvent under reduced pressure, the residue was extracted with ethyl acetate (2×40 mL). The combined organic layers were washed with 10% aqueous $\text{Na}_2\text{S}_2\text{O}_3$ and brine twice, and then dried over Na_2SO_4 . After removal of solvent, the crude product (*R*)-5,5'-dibromo-6,6'-di(4-methylphenyl)-2,2'-binaphthol was purified by column chromatography (petroleum ether/ethyl acetate) (10:1 v/v) to afford a pure solid product (600 mg, 83% yield); Mp: >250 °C; $[\alpha]_{\text{D}} = -70.0$ (*c* 0.5, CH_2Cl_2). ^1H NMR (CDCl_3): δ 8.59–8.62 (d, 2H, $J = 9.3$ Hz), 7.50–7.53 (d, 2H, $J = 9.3$ Hz), 7.32–7.35 (d, 4H, $J = 7.9$ Hz), 7.25–7.27 (d, 6H, $J = 7.2$ Hz), 7.13–7.15 (d, 2H, $J = 8.6$ Hz), 5.14 (s, 2H), 2.42 (s, 6H). ^{13}C NMR (CDCl_3): δ 153.7, 139.6, 139.5, 137.8, 134.0, 132.3, 130.8, 129.9, 129.2, 128.9, 124.0, 123.7, 119.7, 111.3, 21.7. ESI-MS: 623.5 *m/z* ($\text{M} + 1$). Anal. Calcd. for $\text{C}_{34}\text{H}_{24}\text{Br}_2\text{O}_2$: C, 65.38; H, 3.87. Found: C, 65.46; H, 3.77. FT-IR (KBr, cm^{-1}): 3525.8, 3497.6, 3024.1, 2917.2, 1611.0, 1592.1, 1564.1, 1517.5, 1487.4, 1466.4, 1366.7, 1231.9, 1209.8, 1173.8, 1152.2, 1132.1, 1021.6, 955.3, 817.7, 810.9.

A mixture of (*R*)-5,5'-dibromo-6,6'-di(4-methylphenyl)-2,2'-binaphthol (400 mg, 0.64 mmol), K_2CO_3 (710 mg, 5.13 mmol) and *n*- $\text{C}_8\text{H}_{17}\text{Br}$ (500 mg, 2.56 mmol) was dissolved in 20 mL of CH_3CN . The solution was refluxed overnight. After being evaporated to dryness, the residue was extracted with petroleum ether (3×20 mL). The combined organic layers were washed with 5% aqueous NaOH (30 mL) and brine, and then dried over anhydrous Na_2SO_4 . After removal of solvent, the crude product was purified by

chromatography on silica gel with petroleum ether as an eluent to afford a viscous product (*R*)-5,5'-dibromo-6,6'-di(4-methylphenyl)-2,2'-bisoxetoxy-1,1'-binaphthyl (*R*-**M-1**) (540 mg, 99.3% yield); $[\alpha]_{\text{D}} = +29.03$ (*c* 0.62, CH_2Cl_2). ^1H NMR (CDCl_3): δ 8.56 (d, 2H, $J = 9.3$ Hz), 7.54–7.57 (d, 2H, $J = 9.6$ Hz), 7.37–7.39 (d, 4H, $J = 7.8$ Hz), 7.26–7.29 (d, 4H, $J = 7.8$ Hz), 7.14–7.20 (m, 4H), 4.01–4.10 (m, 4H), 2.44 (s, 6H), 1.01–1.27 (m, 24H), 0.88 (t, 6H, $J = 7.1$ Hz). ^{13}C NMR (CDCl_3): δ 155.4, 140.0, 138.6, 137.5, 134.7, 130.0, 129.9, 129.4, 129.0, 128.4, 125.3, 122.9, 120.5, 116.9, 69.9, 32.1, 29.7, 29.6, 26.1, 23.0, 21.7, 14.5. Anal. Calcd. for $\text{C}_{50}\text{H}_{56}\text{Br}_2\text{O}_2$: C, 70.75; H, 6.66. Found: C, 70.79; H, 6.75. FT-IR (KBr, cm^{-1}): 3057.5, 2952.7, 2924.8, 2868.9, 2854.7, 1612.7, 1591.8, 1517.4, 1478.7, 1465.1, 1342.9, 1267.5, 1211.4, 1146.0, 1100.4, 1078.9, 1050.0, 1021.7, 809.2, 708.6.

4.3. Preparation of monomers **M-2** and **M-3**

The monomers **M-2** and **M-3** were prepared and purified as per the reported literatures [22–24,33–36].

M-2 spectroscopic data: Mp: 127–129 °C. ^1H NMR (CDCl_3): δ 5.43 (d, 2H, $J = 10.9$ Hz), 5.92 (d, 2H, $J = 17.6$ Hz), 6.80 (dd, 2H, $J = 17.6, 10.9$ Hz), 7.59 (d, 4H, $J = 8.3$ Hz), 8.12 (d, 4H, $J = 8.3$ Hz). ^{13}C NMR (CDCl_3): δ 116.21, 123.01, 126.78, 127.13, 135.87, 140.82, 164.36. ν_{max} (KBr)/ cm^{-1} : 1625.1, 1577.3, 1492.9, 1411.9, 1080.7, 993.3, 901.9, 851.0, 717.9. MS *m/z*: 274 (M^+ , 82), 131 (100). Elemental anal. (%) Calcd. for $\text{C}_{18}\text{H}_{14}\text{N}_2\text{O}$: C 78.81; H 5.14; N 10.21. Found: C 78.67; H 5.17; N 10.05.

M-3 spectroscopic data: ^1H NMR (CDCl_3): δ 0.92 (t, $J = 7.23$ Hz, 6H), 1.13 (t, $J = 7.8$ Hz, 4H), 1.32–1.42 (m, 4H), 1.53–1.63 (m, 4H), 7.66 (d, $J = 8.1$ Hz, 4H), 8.08 (d, $J = 8.1$ Hz, 4H). ^{13}C NMR (CDCl_3): δ 10.10, 14.53, 27.38, 29.46, 123.79, 126.19, 137.41, 148.48, 165.20. IR, ν_{max} (KBr)/ cm^{-1} : 2956.2, 2926.0, 2870.8, 2832.4, 1599.6, 1535.7, 1483.7, 1463.4, 1052.1, 1015.4, 825.7, 735.0. MS (*m/z*): 801 ($\text{M}^+ + \text{H}$, 100), 362 (27).

4.4. Preparation of polymers **P-1** and **P-2**

A mixture of *R*-**M-1** (159.7 mg, 0.19 mmol) and **M-2** (51.6 mg, 0.19 mmol) was dissolved in the mixed solvents of 5 mL of DMF and 0.3 mL of Et_3N . The solution was first bubbled with N_2 for 15 min before 5 mol% $\text{Pd}(\text{OAc})_2$ (2.2 mg, 0.0098 mmol) and 25 mol% PPh_3 (12.4 mg, 0.047 mmol) were added to the above solution. The temperature of the mixture was kept at 130 °C for 12 h under N_2 , and then refluxed at 140 °C for an additional 2 h. The mixture was cooled to room temperature, and then was filtered through a short silica gel column in methanol (50 mL) to precipitate out the polymer. The resulting polymer was filtered and washed with methanol several times. Further purification could be conducted by dissolving the polymer in CH_2Cl_2 to precipitate in methanol again. **P-1** was dried in vacuum to give 144.9 mg in 80.1% yield. Polymer spectroscopic data: $[\alpha]_{\text{D}} = +154.0$ (*c* 0.10, CH_2Cl_2). ^1H NMR (CDCl_3): 8.53 (br, 2H), 8.16 (br, 4H), 8.07 (br, 2H), 7.50–7.60 (m, 8H), 7.34 (br, 4H), 7.11–7.17

(m, 4H), 6.91–6.96 (m, 4H), 4.02 (br, 4H), 2.40 (s, 6H), 1.47 (br, 4H), 1.08 (br, 20H), 0.84 (s, 6H). Anal. Calcd. for $C_{68}H_{68}N_2O_3$: C, 85.08; H, 7.08; N, 2.92. Found: C, 77.91; H, 7.16; N, 2.65. FT-IR (KBr, cm^{-1}): 3052.0, 3023.4, 2922.5, 2852.9, 1607.7, 1515.6, 1492.3, 1464.1, 1333.9, 1265.7, 1181.3, 1068.9, 1014.8, 961.4, 810.9, 743.7.

P-2 was synthesized by using the Stille reaction. A mixture of **R-M-1** (204.1 mg, 0.24 mmol) and **M-3** (192.4 mg, 0.24 mmol) was dissolved in 8 mL mixed solvents of dioxane and DMF (v/v 1:1). After the solution was bubbled with N_2 for 15 min, $Pd(PPh_3)_4$ (13.9 mg, 0.012 mmol) was added. The reaction solution was kept at 90 °C for 72 h under N_2 . After cooling to room temperature, the solution was filtered through a short silica gel column into methanol (60 mL) to remove palladium black from the solution and precipitate out the crude product **P-2**, which was washed several times with methanol. Further purification could be conducted by dissolving the polymer in CH_2Cl_2 to precipitate in methanol again. **P-2** was dried in vacuum to give 202.4 mg in 87.3% yield. $[\alpha]_D^{25} = +120.0$ (c 0.10, CH_2Cl_2). 1H NMR ($CDCl_3$): 8.29 (br, 2H), 8.18 (br, 2H), 7.92–8.08 (m, 2H), 7.87 (br, 2H), 7.48–7.58 (m, 8H), 7.32–7.36 (m, 4H), 6.98–7.01 (m, 4H), 3.97 (br, 4H), 2.26–2.41 (m, 6H), 1.03–1.19 (m, 4H), 0.84–0.87 (m, 20H), 0.79–0.81 (m, 6H). Anal. Calcd. for $C_{64}H_{64}N_2O_3$: C, 84.58; H, 7.05; N, 3.08. Found: C, 74.11; H, 6.97; N, 3.08. FT-IR (KBr, cm^{-1}): 3054.7, 3023.1, 2923.2, 2853.4, 1612.1, 1591.3, 1516.0, 1496.1, 1482.7, 1343.0, 1265.3, 1183.6, 1093.2, 1075.6, 1019.5, 962.0, 811.8, 733.0.

Acknowledgements

This work was supported by the National Natural Science Foundation of China (no. 20474028), Jiangsu Provincial Natural Science Foundation (no. BK2004086).

References

- Yu WL, Meng H, Pei J, Huang W, Li YF, Heeger AJ. *Macromolecules* 1998;31:4838.
- Bredas JL, Deljonne D, Coropcean V, Cornil J. *Chem Rev* 2004;104:4971.
- Kulkarni AP, Zhu Y, Jenekhe SA. *Macromolecules* 2005;38:1553.
- Hwang SW, Chen Y. *Macromolecules* 2002;35:5438.
- Descalzo AB, Rurack K, Weisshoff H, Ramon MM, Marcos MD, Amoros P, et al. *J Am Chem Soc* 2005;127:184.
- Badugu R, Lakowicz JR, Geddes CD. *J Am Chem Soc* 2005;127:3635.
- Tang YL, Feng FD, He F, Wang S, Zhu DB. *J Am Chem Soc* 2006;128:14972.
- Lu G, Grossman JE, Lambert JB. *J Org Chem* 2006;71:1769.
- Valeur B, Leray IC. *Chem Rev* 2000;205:3.
- De Silva AP, Gunaratne HQN, Gunnlauugsson T, Huxley AJM, McCoy CP, Rademacher JT, et al. *Chem Rev* 1997;97:1515.
- Yasuda T, Yamaguchi I, Yamamoto T. *Adv Mater* 2003;15:293.
- Zhou G, Cheng YX, Wang LX, Jing XB, Wang FS. *Macromolecules* 2005;38:2148.
- Pei J, Liu XL, Yu WL, Lai YH, Niu YH, Cao Y. *Macromolecules* 2002;35:7274.
- Pugh V, Hu QS, Zuo XB, Lewis FD, Pu L. *J Org Chem* 2001;66:6136.
- Pu L. *Chem Rev* 1998;98:2405.
- Li ZB, Lin J, Pu L. *Angew Chem Int Ed* 2005;44:1690.
- Pu L. *Chem Rev* 2004;104:1687.
- Wang D, Liu TJ, Zhang WC. *Chem Commun* 1998;174.
- Meng Y, Williams TS, Wang D, Liu TJ, Chow HJ, Li CJ. *Tetrahedron Asymmetry* 1998;9:3693.
- Sun YM. *Polymer* 2001;42:9495.
- Meer M, Buchwald E, Karg S, Riess W, Greczmiel M. *Synth Met* 1996;76:95.
- Cheng YX, Chen LW, Zou XW, Song JF, Wang ZL. *Polymer* 2006;47:435.
- Song JF, Cheng YX, Chen LW, Zou XW, Wang ZL. *Eur Polym J* 2006;42:663.
- Cheng YX, Chen LW, Song JF, Zou XW, Liu TD. *Polym J* 2005;17:355.
- Qu DH, Wang QC, Jun Ren, Tian H. *Org Lett* 2004;6:2085.
- David GL, Rosario BH, Daniela MZ, Williams DC, Caterina F, Bruno C, et al. *J Med Chem* 2004;47:5612.
- Jens CN, Hanne E. *J Am Chem Soc* 1995;117:1479.
- Lee SJ, Lin WB. *J Am Chem Soc* 2002;124:4554.
- Shi M, Chen LH, Li CQ. *J Am Chem Soc* 2005;127:3790.
- Xu YJ, Clarkson GC, Docherty G, North CL, Woodward G, Wills M. *J Org Chem* 2005;70:8079.
- Ishitani H, Ueno M, Kobayashi S. *J Am Chem Soc* 2000;122:8180.
- Kumaraswamy G, Sastry MNV, Jena N, Kumarb KR, Vairamanic M. *Tetrahedron Asymmetry* 2003;14:3797.
- Zhang JX, Cui YP, Wang ML. *Chem Lett* 2001;824.
- Yin SG, Peng JB, Li CX. *Synth Met* 1998;93:193.
- Chen LW, Liu TD, Cheng YX. *Acta Polym Sinica* 2004;4:590.
- Michael EW. *Organometallics* 1990;9:853.
- Cox PJ, Wang W, Snieckus V. *Tetrahedron Lett* 1992;33:2253.
- Minatti A, Doetz KH. *Tetrahedron Asymmetry* 2005;16:3256.
- Wu TR, Shen L, Chong JM. *Org Lett* 2004;6:2701.
- Shimada T, Suda M, Nagano T, Kakiuchi K. *J Org Chem* 2005;70:10178.
- Alame M, Jahjah M, Berthod M, Lemaire M, Meille V, Bellefon C. *J Mol Catal A Chem* 2007;268:205.
- Pirkle WH, Schreiner JL. *J Org Chem* 1981;46:4988.
- Tian Y, Yang QC, Mak TCW, Chan KS. *Tetrahedron* 2002;58:3951.
- Tian Y, Chan KS. *Tetrahedron Lett* 2000;41:8813.
- Hu QS, Pugh V, Sabat M, Pu L. *J Org Chem* 1999;64:7528.
- Lee SJ, Hu A, Lin WB. *J Am Chem Soc* 2002;124:12948.
- Zhu YL, Gergel N, Majumdar N, Harriott LR, Bean JC, Pu L. *Org Lett* 2006;8:355.
- Cui Y, Ewans OR, Ngo HL, White PS, Lin W. *Angew Chem Int Ed* 2002;41:1159.
- Meijere A, Meyer FE. *Angew Chem Int Ed Engl* 1994;33:2379.
- Cheng YX, Liu TD, Chen LW. *Chin J Chem* 2003;21:1101.
- Zhang HC, Pu L. *Tetrahedron* 2003;59:1703.
- Scherf U, Mullen K. *Synthesis* 1992;1–2:23.
- Su W, Urgaonkar S, McLaughlin PA, Verkade JG. *J Am Chem Soc* 2004;126:16433.
- Roussel S, Abarbri M, Thibonnet J, Parrain JL, Duchêne A. *Tetrahedron Lett* 2003;44:7633.
- Kelvin CYL, Pauline C. *Tetrahedron Lett* 2007;48:1813.
- Zheng L, Urian RC, Liu Y, Jen AKY, Pu L. *Chem Mater* 2000;12:13.
- Peng ZH, Bao ZN, Galvin ME. *Adv Mater* 1998;10:680.
- Zhang HC, Pu L. *Macromolecules* 2004;37:2695.
- Cheng YX, Song JF, Zou XW, Zhang SW, Liu Y, Huang H. *Polymer* 2006;47:6598.
- Chow HF, Ng MK. *Tetrahedron Asymmetry* 1996;7:2251.
- Kokil A, Yao P, Weder C. *Macromolecules* 2005;38:3800.
- Kimura M, Horai T, Hanabusa K, Shirai H. *Adv Mater* 1998;10:459.
- Murphy CB, Zhang Y, Troxler T, Ferry V, Martin JJ, Jones WE. *J Phys Chem B* 2004;108:1537.
- Chen LX, Jäger WJH, Gosztola DJ, Niemczyk MP, Wasielewski MR. *J Phys Chem B* 2000;104:1950.